Transport Analysis of Diffusion-Induced Bubble Growth and Collapse in Viscous Liquids

David C. Venerus and Nadia Yala
Dept. of Chemical Engineering and Environmental Engineering,
Center of Excellence in Polymer Science and Engineering, Illinois Institute of Technology, Chicago, IL 60616

Transport models of diffusion-induced bubble growth and collapse in viscous liquids are developed and evaluated. A rigorous model for these important phenomena is formulated taking into account convective and diffusive mass transport, surface tension, and viscous and inertial effects. Predictions for bubble growth dynamics demonstrate the importance of viscous effects in the liquid surrounding the bubble for a wide range of conditions having relevance to polymer processing operations. It is also shown how previous models employing various approximations can be derived from the rigorous model by using different mathematical methods and dimensional analysis. Predicted bubble growth dynamics from the rigorous and approximate models are compared to establish the ranges of validity for two commonly used approximations. These comparisons indicate that models using a thin boundary-layer approximation have a rather limited range of applicability. A new approximate model, based on a previously published result, gives reasonably accurate bubble growth rate predictions with a significant reduction in computational effort.

Introduction

The mass diffusion-induced growth and collapse of gas bubbles in liquids occurs in numerous chemical and materials processing operations. Not surprisingly, many studies have been conducted in order to develop transport models that allow prediction of bubble growth or collapse rates, which, in turn, can be used to design process equipment or to interpret experiments designed to measure transport properties. In many situations, the disparate time scales for mass and momentum transport in the liquid surrounding the bubble allow the two transport processes to be decoupled. For slow growth or dissolution of bubbles in low viscosity liquids, momentum transport in the liquid can often be neglected; and the rate of bubble growth or collapse is controlled by the rate of mass diffusion. However, in situations where the liquid surrounding the bubble has a relatively high viscosity, momentum transfer in the liquid can significantly influence mass transfer. For example, in the production of polymeric foams and in polymer devolatilization processes, the high viscosity of the molten polymer surrounding the bubble can have substantial effects on the rate of bubble growth and collapse (Villamizar and Han, 1978; Han and Yoo, 1981). In this study, we will primarily be concerned with modeling the isothermal growth and collapse of a single, spherical, gas bubble surrounded by a viscous liquid of infinite extent where the growth or collapse is the result of an externally-imposed concentration difference of a diffusing species.

The transport modeling of mass diffusion-controlled bubble growth and collapse has received a great deal of attention and one could argue that it is fairly well developed from a theoretical point of view. While the decoupling of momentum transport from mass transport results in a considerable degree of simplification, the governing equations constitute a nonlinear, moving boundary problem for which no exact analytical solutions are available. Numerical solutions of the governing equations using finite difference methods have been reported where the difficulties of a moving boundary, steep concentration gradients, and an infinite domain encountered in this problem have been resolved (Duda and Vrentas, 1969). Approximate analytical solutions have been found for rapid or slow growth and dissolution rates using perturbation techniques (Epstein and Plesset, 1950; Duda and Vrentas, 1969) and thin boundary-layer approximations (Plesset and Zwick,

Correspondence concerning this article should be addressed to D. C. Venerus.

1952; Rosner and Epstein, 1972). A summary of approximate analytical solutions of diffusion-controlled bubble growth and collapse problems and recommendations for their use is available (Vrentas et al., 1983). For the case of bubble growth from a zero initial radius, an exact solution based on similarity transformation has been found (Scriven, 1959).

The development of transport models for diffusion-*induced* bubble growth and collapse in viscous liquids involves additional, and sometimes subtle, effects not found in the governing equations for diffusion-*controlled* phenomena. The transport equations governing diffusion-controlled bubble growth and collapse must be modified and augmented with a mass balance on the gas bubble and a momentum balance on the liquid surrounding the bubble, which are coupled by boundary conditions at the gas-liquid interface that take on somewhat different forms.

Surprisingly, a rigorous formulation of the governing equations for diffusion-induced bubble growth or collapse has not been previously published. All previous analysis of this transport problem is based on the use of approximations that simplify the model considerably. While model simplicity is, of course, desirable, the validity of these approximations has yet to be established. One approximation is founded on the argument that the driving force for mass diffusion, based on the difference between the initial concentration of the diffusing species and the concentration at saturation, is small, We shall refer to this as the infinitely dilute solute (IDS) approximation. The second is the well-known thin boundary layer (TBL) approximation, which assumes that variations in the concentration of the diffusing species are confined to a thin region surrounding the bubble.

Here, we briefly summarize previous studies where the problem of diffusion-induced bubble growth or collapse in viscous liquids has been analyzed. Apparently, the first analysis was carried out by Barlow and Langlois (1962) who considered the growth of a gas bubble surrounded by a Newtonian liquid. This analysis invokes a TBL approximation based on the work of Plesset and Zwick (1952), and also makes use of the IDS approximation. The TBL approximation used by Plesset and Zwick (1952) can be regarded as a perturbation solution in which the volume of the concentration boundary layer is assumed to be small compared to the volume of the growing bubble. Street et al. (1971) followed the same development as Barlow and Langlois and developed a model for nonisothermal bubble growth in a non-Newtonian fluid of the power-law type. At about the same time, Szekely and Martins (1971) developed a model for bubble growth in a Newtonian liquid in which the IDS and other approximations were utilized. The dissolution of a gas bubble in a Newtonian liquid and in a viscoelastic liquid (Oldroyd B fluid) was modeled by Zana and Leal (1975) who also used the IDS approximation. A model for bubble growth in a Newtonian liquid was developed by Patel (1980) based on a TBL approximation used by Rosner and Epstein (1972), which also used the IDS approximation. The TBL approximation used by Rosner and Epstein (1972), who developed a model for bubble growth in which viscous and inertial effects were neglected, can be classified as a special type of weighted residuals method where the species continuity equation is satisfied only in an average sense. Patel found that predictions from this model were in good agreement with those obtained by Barlow and Langlois (1962). Han and Yoo (1981) developed a model using a TBL approximation similar to that of Rosner and Epstein (1972) and the IDS approximation to describe the growth of a bubble in a Newtonian fluid and in a corotational Maxwell (viscoelastic) fluid. The early-time dynamics of bubble growth and collapse in Newtonian and viscoelastic liquids were also examined using the same transport model (Yoo and Han, 1982). A model for bubble growth in liquids has also been developed using a weighted residuals method similar to Rosner and Epstein (1972) that did not require a TBL approximation (Payvar, 1987). It should be noted, however, that the model developed by Payvar (1987) excluded viscous, inertial and surface tension effects. More recently, Ramesh et al. (1991) used a model similar to Han and Yoo (1981) to describe bubble growth in power law and Maxwell model fluids.

As noted above, this study is concerned with transport modeling of the growth and dissolution of a bubble surrounded by a liquid of infinite extent where, because of the unlimited amount of diffusing species, the bubble will grow indefinitely or collapse completely. A number of models have been developed in which the bubble is surrounded by a fictitious liquid shell of finite size. Since the amount of diffusing species is finite, the bubble radius approaches a terminal value that depends on the assumed size of the initial liquid shell. While there appears to be a connection between the finite shell model and the TBL approximation models mentioned above, fundamentally they are different in that the former predicts a terminal bubble radius while the latter predicts indefinite bubble growth. Amon and Denson (1984) appear to be the first to have used this approach to describe the growth of a bubble surrounded by a finite shell of a Newtonian liquid. Arefmanesh et al. (1992) developed a similar model and made comparisons of predicted bubble growth to those from the TBL approximation model of Rosner and Epstein (1972) and Patel (1980). The results of such a comparison are somewhat inconclusive since the bubble radius at all but early stages of the growth process predicted by the finite shell model can be strongly influenced by the approach of the bubble radius to its terminal value. The finite shell model was also used by Arefmanesh and Advani (1991) to describe the growth of a bubble in an upper convected Maxwell (viscoelastic) fluid. It should be noted that in all of the finite shell models mentioned here, the IDS approximation was utilized.

Hence, in all previous studies on bubble growth or collapse in viscous liquids, either the infinitely dilute solute approximation, or a thin boundary layer approximation, or both, have been used. Moreover, a number of models where more complicated effects such as fluid elasticity have been included (Han and Yoo, 1981; Ramesh et al., 1991), and a model for predicting bulk flow in polymer foam processing (Arefmanesh et al., 1990), are based on transport models using both approximations, neither of which have been justified. Intuitively, one would expect viscous effects in the liquid surrounding the bubble to retard the rate of growth or dissolution in comparison with the diffusion-controlled case. Indeed, this is what has been reported in previous analysis of this problem. While much has been gained from the studies mentioned above, it appears that further progress in this area would be facilitated by formulating a rigorous transport model so that conditions for the validity of the approximations used in all previous models can be established. In the following section, we formulate a rigorous transport model for the diffusion-induced growth and collapse of a gas bubble in a viscous liquid. From this rigorous model, we derive previously published, approximate models of these phenomena. In the third section of this article, we present comparisons of bubble growth dynamics from the rigorous model with those obtained from the approximate models and discuss the appropriateness of the approximations used to derive the latter. A simple, but accurate approximate model is also developed and evaluated. In the final section, the findings of this study are summarized.

Problem Formulation

In this section, we first give the assumptions that are used in formulating the problem of diffusion-induced bubble growth and collapse in a viscous liquid. Rigorous forms of the governing transport equations are presented in dimensionless form. It is then demonstrated how this set of equations can be manipulated into simplified forms that have been considered in previous work on this problem.

Consider the growth of a single-component, spherical gas bubble surrounded by a liquid of infinite extent. The liquid is of binary constitution: one component is a volatile species from which the bubble is composed, and the other component is a nonvolatile species. The entire system is assumed to be isothermal, and there are no chemical reactions. Mass diffusion is assumed to be governed by Fick's law with a constant diffusivity D. The position of the bubble is fixed and located at the origin of a spherical coordinate system. The gas within the bubble is assumed to be inviscid and to obey the ideal gas law. If inertial effects in the bubble are also neglected, the pressure within the bubble will be uniform. It also assumed that equilibrium exists at the gas-liquid interface and is governed by Henry's law with Henry's law constant k.

In the liquid surrounding the bubble, it is assumed that the velocity field is purely radial and that the solute concentration field is spherically symmetric. The liquid surrounding the bubble is assumed to be an incompressible Newtonian fluid with constant viscosity μ and constant mass density ρ. All the gravitational effects are neglected, and the pressure far from the bubble is assumed be constant at p_∞. In addition, the interfacial tension at the gas-liquid interface is assumed to be σ. Initially, the bubble has radius R_0, and is surrounded by a liquid at rest with a uniform solute mass density (mass solute/volume of mixture) of ρ_{10} and a uniform pressure of p_∞.

Rigorous model

We now give the dimensionless form of the governing equations that define the transport problem. Definitions for the dimensionless variables and the dimensional quantities used to define them can be found at the end of this article. We note here, however, that R_0 is the characteristic length and R_0^2/D is the characteristic time, which is consistent with the scheme typically used to model diffusion-*controlled* behavior. The species continuity equation for the mass density of the volatile species $\rho_1 = \rho_1(r,t)$ is given by

$$\frac{\partial \rho_1}{\partial t} + v_r \frac{\partial \rho_1}{\partial r} = \frac{1}{r^2}\frac{\partial}{\partial r}\left(r^2 \frac{\partial \rho_1}{\partial r}\right) \tag{1}$$

Total mass continuity in the liquid allows the radial component of the mass-average velocity $v_r = v_r\,(r,t)$ to be written as

$$v_r = \frac{f(t)}{r^2} \tag{2}$$

where f is a dimensionless function of time. The initial and boundary conditions for Eq. 1 are given by

$$\rho_1(r,0) = 0 \tag{3}$$

$$\rho_1(\infty,t) = 0 \tag{4}$$

$$\rho_1(R,t) = \frac{1 - N_K p_g}{1 - N_K} \tag{5}$$

where $R = R(t)$ is the bubble radius, and $p_g = p_g(t)$ is the pressure within the gas bubble. Jump mass balances at the gas-liquid interface allow the function $f(t)$ in Eq. 2 to be expressed as follows

$$f = R^2\left[\frac{dR}{dt} + N_B \frac{1 - N_K}{1 - N_K - N_B N_K (p_g - 1)}\left(\frac{\partial \rho_1}{\partial r}\right)_{r=R}\right] \tag{6}$$

A total mass balance on the gas bubble can be written as

$$\frac{d}{dt}\left(p_g R^3\right) = -3R^2 N_A \frac{1 - N_K}{1 - N_K - N_B N_K (p_g - 1)}\left(\frac{\partial \rho_1}{\partial r}\right)_{r=R} \tag{7}$$

The radial component of the Navier-Stokes equations can be integrated over the radial coordinate from R to ∞; combined with the jump linear momentum balance at the gas-liquid interface, to give

$$p_g = 1 + 2\frac{N_C}{R} + 4N_T\frac{f}{R^3} + N_R\left[\frac{1}{R}\frac{df}{dt} - \frac{f^2}{2R^4}\right] \tag{8}$$

Equation 8 shows that the pressure within the bubble deviates from its (dimensionless) value of one as a result of surface tension, viscous and inertial forces. It is clear that variations of p_g couple momentum transfer to the mass-transfer process via the boundary condition, Eq. 5, *and* via the convective mass transport process, Eq. 6. The initial conditions for Eqs. 6–8 are given by

$$R(0) = 1 \tag{9}$$

$$p_g(0) = 1 + 2N_C \tag{10}$$

$$f(0) = 0 \tag{11}$$

Equations 1–11 constitute the rigorous transport model for diffusion-induced bubble growth and collapse in viscous liquids, which apparently have not been previously published.

Table 1. Dimensionless Groups and Their Values

$N_A = \left(\dfrac{\rho}{Ap_\infty}\right)\dfrac{\rho_{10} - kp_\infty}{\rho - kp_\infty}$	1, 10, 100
$N_B = \dfrac{\rho_{10} - kp_\infty}{\rho - kp_\infty}$	$10^{-3}\ N_A$
$N_K = \dfrac{kp_\infty}{\rho_{10}}$	0.01
$N_C = \dfrac{\sigma}{p_\infty R_0}$	0.4
$N_T = \dfrac{\mu D}{p_\infty R_0^2}$	0, 0.1, 1.0, 10
$N_R = \dfrac{\rho D^2}{p_\infty R_0^2}$	$10^{-6}\ N_T$

Clearly, this coupled set of equations is nonlinear and it is unlikely that an exact analytical solution can be found.

The six dimensionless groups (N_A, N_B, N_C, N_K, N_R, N_T) that appear in Eqs. 1–11 are defined in Table 1. The group N_B is a dimensionless concentration difference, or driving force for mass diffusion. The group N_A is this same driving force scaled by the ratio of the liquid density to a characteristic gas bubble density. The magnitude of N_A is an indication of the rate of growth or collapse; the difference $|N_A - N_B|$ is a measure of the importance of convective mass transport. Both N_A and N_B are positive for bubble growth and negative for bubble collapse; for the growth and collapse of gas bubbles in liquids under typical conditions, $|N_B| \ll |N_A|$. The group N_K is a dimensionless Henry's law constant and for nonzero values of N_A and N_B, $N_K \neq 1$. The ratio of characteristic times for viscous momentum and diffusive mass transport is indicated by N_T. The ratio of characteristic times for inertial momentum and diffusive mass transport is given by N_R. Finally, the group N_C is a dimensionless surface tension.

Before we consider the approximations used to simplify the rigorous model defined by Eqs. 1–11, we show under what conditions the diffusion-controlled limit is achieved. If viscous, inertial, and surface tension forces are neglected ($N_T \to 0$, $N_R \to 0$, $N_C \to 0$), Eq. 8 becomes

$$p_g = 1 \tag{12}$$

so the boundary condition at the gas-liquid interface, Eq. 5, becomes

$$\rho_1(R,t) = 1 \tag{13}$$

and Eqs. 6 and 7 can be written as

$$f = -R^2(N_A - N_B)\left(\frac{\partial \rho_1}{\partial r}\right)_{r=R} \tag{14}$$

$$\frac{dR}{dt} = -N_A\left(\frac{\partial \rho_1}{\partial r}\right)_{r=R} \tag{15}$$

Equations 1–4, 9, and 13–15 constitute the governing equations for diffusion-*controlled* bubble growth or collapse and contain the two dimensionless groups N_A and N_B. [(The dimensionless groups N_a and N_b used by Vrentas et al. (1983) are related to those used here by replacing kp_∞ with ρ_{1e}, the equilibrium solute mass density; replacing Ap_∞ with ρ_g, the gas bubble density; and noting: $N_a = -N_A$ and $N_b = -N_B$.)] There are no known exact solutions for this transport problem. For bubble growth from a zero initial radius bubble, $R(0) = 0$, Eqs. 1–4 and 13–15 admit an exact similarity solution of the form

$$R = 2\beta\sqrt{t} \tag{16}$$

where β is a constant that depends on the values of N_A and N_B (Scriven, 1959).

It has been noted (Vrentas et al., 1983) that numerical solutions of Eqs. 1–4, 9, and 13–15 are in good agreement with the similarity solution given in Eq. 16 for $R \gtrsim 5$. Hence, for diffusion-controlled bubble growth from a nonzero initial radius bubble where $R \gtrsim 5$, $dR/d\sqrt{t}$, which we will refer to as the rate of bubble growth, is constant. Physically, this occurs because the concentration boundary layer thickness increases at the same rate as the bubble radius. It is also evident that when $R \to \infty$, Eq. 8 reduces to Eq. 12. Consequently, even if viscous, inertial and surface tension forces are significant during early stages of bubble growth, diffusion-controlled behavior is always reached in the limit $R \to \infty$. In other words, the bubble growth rate (that is, $dR/d\sqrt{t}$) will asymptotically approach the same constant value as for diffusion-controlled growth.

Approximate models

We now consider a model that uses the infinitely dilute solute (IDS) approximation, which will be valid when $|N_B| \ll 1$. Setting $N_B = 0$ allows Eq. 6 to be written as

$$f = R^2\frac{dR}{dt} \tag{17}$$

The radial component of the velocity field is, combining Eqs. 2 and 17, given by

$$v_r = \frac{R^2}{r^2}\frac{dR}{dt} \tag{18}$$

The particularly simple result given in Eq. 18 *is valid in a strict sense only if there is no mass transfer across the gas-liquid interface*; when there is mass transfer across the interface, it is valid only if $N_B/N_A \ll 1$, which is consistent with the IDS approximation, $|N_B| \ll 1$, as long as the growth or collapse rate is not large. Substitution of Eq. 18 in Eq. 1 gives

$$\frac{\partial \rho_1}{\partial t} + \frac{R^2}{r^2}\frac{dR}{dt}\frac{\partial \rho_1}{\partial r} = \frac{1}{r^2}\frac{\partial}{\partial r}\left(r^2\frac{\partial \rho_1}{\partial r}\right) \tag{19}$$

Setting $N_B = 0$ allows Eq. 7 to be written as

$$\frac{d}{dt}\left(p_g R^3\right) = -3R^2 N_A\left(\frac{\partial \rho_1}{\partial r}\right)_{r=R} \tag{20}$$

Substitution of Eq. 17 in Eq. 8 gives

$$p_g = 1 + 2\frac{N_C}{R} + 4N_T\frac{1}{R}\frac{dR}{dt} + N_R\left[R\frac{d^2R}{dt^2} + \frac{3}{2}\left(\frac{dR}{dt}\right)^2\right] \quad (21)$$

where the initial condition given in Eq. 11 is replaced by

$$\frac{dR}{dt}(0) = 0 \quad (22)$$

Hence, using the IDS approximation ($|N_B| \ll 1$), the growth or dissolution of a gas bubble in a viscous liquid is governed by Eqs. 19–21 with boundary and initial conditions given in Eqs. 3–5, 9, 10 and 22 and the five dimensionless groups N_A, N_C, N_K, N_R, N_T. This is similar to the model proposed previously by Szekely and Martins (1971), although a somewhat different form of Eq. 20 was considered. [Szekely and Martins (1971) used the following expression in place of Eq. 20 $p_g(dR/dt) = -N_A(\partial\rho_1/\partial r)_{r=R}$.]

The second approximation frequently used in models for diffusion-induced bubble growth is the thin-boundary layer (TBL) approximation. The TBL approximation assumes that the variation of the concentration field is confined to a thin shell surrounding the bubble. Physically, this approximation implies that the rate of growth of the concentration boundary layer is small compared to the rate of bubble growth and, consequently, should be applicable for rapid growth situations: $N_A \gg 1$. For diffusion-controlled bubble growth, it has been noted that TBL models are valid for $N_A \geq 10$ (Vrentas et al., 1983). The TBL approximation has been implemented in diffusion-induced bubble growth models using two different mathematical approaches.

First, we consider the method developed by Plesset and Zwick (1952), which can be thought of as a perturbation method where the ratio of concentration boundary layer volume to bubble volume serves as the perturbation parameter. This approach is based on a change of variables

$$\xi = \frac{1}{3}[r^3 - R(t)^3] \quad (23)$$

$$\tau = \int_0^t R(t')^4\, dt' \quad (24)$$

where ξ can be thought of as a Lagrangian radial coordinate, and τ is transformed time. More importantly, $4\pi\xi$ is assumed to be the volume of the concentration boundary layer so that the perturbation parameter (the ratio of concentration boundary layer volume to bubble volume) is given by $3\xi/R^3$. Application of the change in variables given by Eqs. 23 and 24 in Eqs. 1, 2, 6 and 7, combining them and using the inequality $3\xi/R^3 \ll 1$, gives

$$\frac{\partial\rho_1}{\partial\tau} - \frac{N_B}{3N_AR^2}\frac{d}{dt}\left(p_gR^3\right)\frac{\partial\rho_1}{\partial\xi} = \frac{\partial^2\rho_1}{\partial\xi^2} \quad (25)$$

Clearly, the nonlinear convective term drops out only when $N_B/N_A \ll 1$, and in such cases, Eq. 25 can be written as

$$\frac{\partial\rho_1}{\partial\tau} = \frac{\partial^2\rho_1}{\partial\xi^2} \quad (26)$$

The initial and boundary conditions for Eq. 26 are the following

$$\rho_1(\xi,0) = 0 \quad (27)$$

$$\rho_1(\xi,\tau) = 0 \quad \text{for} \quad 3\xi \ll R^3 \quad (28)$$

$$\rho_1(0,\tau) = \frac{1 - N_Kp_g}{1 - N_K} \quad (29)$$

Equations 26–29 constitute a linear boundary value problem for which an analytical solution can be found in terms of the unknown bubble radius $R(t)$ and gas pressure $p_g(t)$. This solution can be used to evaluate the righthand side of Eq. 20. Hence, the problem can be reduced to the solution of two nonlinear, ordinary differential equations for $R(t)$ and $p_g(t)$, Eqs. 20 and 21, subject to the initial conditions given in Eqs. 9, 10 and 22. Using this method, Barlow and Langlois (1962) derived a single, nonlinear integro-differential equation for $R(t)$. Note that this approach for implementing the TBL approximation also makes use of the IDS approximation. Since the TBL approximation implies $N_A \gg 1$ and the IDS approximation implies $N_B \ll 1$, it appears that this model for bubble growth in liquids, where $N_B/N_A \sim 10^{-3}$, will have a fairly narrow range of applicability.

The second method for introducing the TBL approximation is the integral or moment method, and is a special type of weighted residuals method (Rosner and Epstein, 1972). This method involves postulating a functional form for the concentration field in terms of an unknown function of time, in this case, the thickness of the concentration boundary layer, $\delta(t)$. First, Eq. 1 is multiplied by r^2 and integrated over the radial coordinate from R to $R+\delta$; it is combined with Eqs. 2 and 5–7. Use is then made of the following properties of the assumed concentration field: $(\rho_1)_{R+\delta} = 0$; $(\partial\rho_1/\partial r)_{r=R+\delta} = 0$. Finally, the result of this procedure is integrated over time with Eqs. 3, 9 and 10 to give the following expression

$$\int_R^{R+\delta} r^2\rho_1 dr = \frac{1 - N_B}{3N_A}\left[p_gR^3 - (1 + 2N_C)\right] \quad (30)$$

Rosner and Epstein (1972) assumed the following form for the concentration field

$$\rho_1(r,t) = \frac{1 - N_Kp_g}{1 - N_K}\begin{cases}\left(1 - \dfrac{r-R}{\delta}\right)^2 & R \leq r \leq R+\delta \\ 0 & r \geq R+\delta\end{cases} \quad (31)$$

From Eq. 31 we have

$$\left(\frac{\partial\rho_1}{\partial r}\right)_{r=R} = -2\frac{R}{\delta}\left(\frac{1 - N_Kp_g}{1 - N_K}\right)\frac{1}{R} \quad (32)$$

and substitution of Eq. 31 in the lefthand side of Eq. 30 gives after integrating

$$\frac{\delta}{R}+\frac{1}{2}\left(\frac{\delta}{R}\right)^{2}+\frac{1}{10}\left(\frac{\delta}{R}\right)^{3}=\frac{1-N_B}{N_A}\left[\frac{1-N_K}{1-N_K\rho_g}\right]\frac{\rho_g R^3-(1+2N_C)}{R^3} \qquad (33)$$

Retaining only the first term on the lefthand side of Eq. 33, that is, for $\delta/R \ll 1$; combining this result with Eqs. 7 and 32 gives the following expression

$$\frac{d}{dt}\left(\rho_g R^3\right)=\frac{6N_A^2(1-N_K\rho_g)^2 R}{(1-N_B)(1-N_K)[1-N_K-N_BN_K(\rho_g-1)]}\times\frac{R^3}{\rho_g R^3-(1+2N_C)} \qquad (34)$$

It has been suggested (Han and Yoo, 1981) that the accuracy of the TBL approximation can be improved if the first and second terms on the lefthand side of Eq. 33 are retained and the resulting quadratic equation is solved for δ/R. This result, combined with Eqs. 7 and 32 gives

$$\frac{d}{dt}\left(\rho_g R^3\right)=\frac{6N_A(1-N_K\rho_g)R}{1-N_K-N_BN_K(\rho_g-1)}\times\left(\sqrt{1+2\frac{1-N_B}{N_A}\frac{1-N_K}{1-N_K\rho_g}\frac{\rho_g R^3-(1+2N_C)}{R^3}}-1\right)^{-1} \qquad (35)$$

The integral method developed by Payvar (1987) employed the following functional form for the concentration field in the boundary layer in place of the one given in Eq. 31

$$\rho_1(r,t)=\frac{1-N_K\rho_g}{1-N_K}\begin{cases}\dfrac{R}{r}\left(1-\dfrac{r-R}{\delta}\right)^2 & R\le r\le R+\delta\\ 0 & r\ge R+\delta\end{cases} \qquad (36)$$

From Eq. 36 we have

$$\left(\frac{\partial\rho_1}{\partial r}\right)_{r=R}=-\left(1+2\frac{R}{\delta}\right)\left(\frac{1-N_K\rho_g}{1-N_K}\right)\frac{1}{R} \qquad (37)$$

and substitution of Eq. 36 in the lefthand side of Eq. 30 gives after integrating

$$\frac{\delta}{R}+\frac{1}{4}\left(\frac{\delta}{R}\right)^{2}=\frac{1-N_B}{N_A}\left[\frac{1-N_K}{1-N_K\rho_g}\right]\frac{\rho_g R^3-(1+2N_C)}{R^3} \qquad (38)$$

Solution of Eq. 38 for δ/R and combination with Eqs. 7 and 37, gives

$$\frac{d}{dt}\left(\rho_g R^3\right)=\frac{3N_A(1-N_K\rho_g)R}{1-N_K-N_BN_K(\rho_g-1)}\times\left[1+\left(\sqrt{1+\frac{1-N_B}{N_A}\frac{1-N_K}{1-N_K\rho_g}\frac{\rho_g R^3-(1+2N_C)}{R^3}}-1\right)^{-1}\right] \qquad (39)$$

As noted by Payvar (1987), this approximate solution of the species continuity equation is not restricted to small values of δ/R. Consequently, the result given in Eq. 39 should not be considered a TBL approximation and should be valid for all values of N_A.

The integral method has been used to find approximate solutions of Eqs. 1–6, which has resulted in three different expressions for the mass balance on the gas bubble: Eqs. 34, 35 and 39. It should be noted that the equations given in Eqs. 34, 35 and 39 are all singular at $t=0$, and, consequently, will require special integration techniques. The singularity in Eq. 34 can be eliminated using a simple change of variable. [The following change of variable suggested by Patel (1980) can be used to resolve the singularities in Eqs. 34 and 41: $\sqrt{x}=\rho_g R^3-(1+2N_C)$.] The change of variable required to resolve the singularity in Eq. 35 or 39 is not, however, obvious. Here, we only consider the TBL approximation derived by Rosner and Epstein (1972) (Eq. 34), which has been the basis for several studies on bubble growth modeling. In the following section, a comparison of all three approximate solutions with the exact similarity solution will be made. Combination of Eqs. 6, 32 and 33, for $\delta/R \ll 1$, gives

$$f=R^2\frac{dR}{dt}-2\frac{N_AN_B}{1-N_B}\times\frac{(1-N_K\rho_g)^2}{(1-N_K)[1-N_K-N_BN_K(\rho_g-1)]}\frac{R^4}{\rho_g R^3-(1+2N_C)} \qquad (40)$$

Hence, Eqs. 8–11, 34 and 40 constitute a TBL approximation model derived using the integral model of Rosner and Epstein (1972).

As discussed in the previous section, several studies on bubble growth have used both the TBL approximation based on the integral method and the IDS approximation (Patel, 1980; Han and Yoo, 1981; Ramesh et al., 1991). In order to reproduce these models, Eq. 40 must reduce to Eq. 17, which can be achieved if $|N_AN_B/(1-N_B)|\ll 1$; and Eq. 34 must simplify to

$$\frac{d}{dt}\left(\rho_g R^3\right)=6N_A^2\left[\frac{1-N_K\rho_g}{1-N_K}\right]^2\frac{R^4}{\rho_g R^3-(1+2N_C)} \qquad (41)$$

which will be true since $N_B \ll 1$. Hence, integration of Eqs. 21 and 41 with initial conditions given in Eqs. 9, 10 and 22 constitute a model for bubble growth in which both the TBL and IDS approximations are used. Use of these two approximations will, as noted earlier, result in a fairly narrow range of applicability for this model.

We now summarize the transport models derived above that will be compared in the following section. The rigorous model for bubble growth and collapse in viscous liquids is defined by Eqs. 1–11. The model for bubble growth and collapse using the IDS approximation ($|N_B| \ll 1$) is given by solution of Eqs. 3–5, 9, 10 and 19–22. Two methods for introducing the TBL approximation in models for describing bubble growth in viscous liquids have been discussed—the perturbation method and the integral method. The IDS approximation has also been used in models where the TBL approximation has been introduced by the perturbation method (Barlow and Langlois, 1962; Street et al., 1971) and by the integral method (Patel, 1980; Han and Yoo, 1981); it has been shown (Patel, 1980) that the two models give similar results. Hence, we shall consider only the model derived using the integral method for introducing the TBL approximation along with the IDS approximation, which is given by solution of Eqs. 9, 10, 21, 22 and 41.

Results and Discussion

In this section, we present and compare predicted bubble growth dynamics from the rigorous and approximate models derived in the previous section. Also, a new approximate model is proposed and evaluated.

The models presented above are all highly nonlinear and, consequently, require numerical solution. In models requiring solution of the species continuity equation, an implicit finite difference method was used. Before discretization, a coordinate transformation was applied (Duda and Vrentas, 1969) to immobilize the moving boundary and map the infinite domain into a finite one. The code was first checked by solving diffusion-controlled bubble growth problems ($p_g = 1$) and comparing the computed $R(t)$ results with previously published results (Duda and Vrentas, 1969) and with results from the exact similarity solution for $R \gg 1$. For the rigorous and IDS approximation models of diffusion-induced bubble growth and collapse ($p_g \neq 1$), the spatially-discretized form of the species continuity equation was solved using the method of lines so that simultaneous integration of the ordinary differential equations for $R(t)$, $p_g(t)$ and $f(t)$ was possible. For the model using both the IDS and TBL approximations, solution of the ordinary differential equations for $R(t)$ and $p_g(t)$ was carried out using standard integration routines. Convergence of the numerical solutions was insured by refining the spatial and temporal step sizes.

As noted in the previous section, six dimensionless groups (see Table 1) appear in the rigorous model for bubble growth and collapse in viscous liquids. Clearly, systematic study of all these groups to determine their influence on bubble growth dynamics would not be practical. Therefore, we have chosen to focus on a subset of the six groups that are likely to have the highest degree of variability in systems of practical importance, and that will have bearing on the approximations used in previously proposed models. Values of the dimensionless groups used in this study and shown in Table 1 were determined from data given in previous bubble growth studies (Barlow and Langlois, 1962; Han and Yoo, 1981) that have focused on the growth of bubbles in polymer liquids containing a dissolved, low molecular weight species.

The group N_A ($=1$, 10, 100) will be examined in some detail since its magnitude controls the rate of bubble growth and is connected to the validity of the TBL approximation. The group N_B will also be studied since it is related to the IDS approximation. As shown in Table 1, the ratio of N_B/N_A, which equals the ratio of a characteristic gas bubble density to liquid density, will be held constant at a value of 10^{-3}. The second dimensionless group to be considered in detail is N_T ($=0$, 0.1, 1.0, 10), which indicates the relative importance of viscous effects in the liquid surrounding the bubble. Due to the relatively high viscosity of molten polymers, $N_R \ll 1$ as indicated in Table 1, and, consequently, inertial effects are effectively neglected. The dimensionless Henry's law constant N_K and the dimensionless surface tension N_C were fixed at the values shown in Table 1 that are typical for gas-bubble/polymer-liquid systems.

Rigorous model predictions

We first consider predictions from the rigorous model for bubble growth and examine the effect of viscous forces in the liquid surrounding the bubble. Figure 1 shows bubble growth dynamics for $N_A = 10$ and different values of N_T in terms of the bubble radius R vs. $\sqrt{t}$. From this figure, it is evident that as N_T is increased, bubble growth is retarded compared with the diffusion-controlled case (dashed line). Figure 1 also shows that at later stages of the growth process, the rate of bubble growth approaches the rate of diffusion-controlled growth; that the time (or bubble sized) required to reach a constant growth rate increases with increasing N_T.

Figure 2 shows bubble pressure dynamics for the same cases shown in Figure 1. For the three values of N_T shown in Figure 2, the bubble pressure increases from its initial value, goes through a maximum, and then gradually approaches the bubble pressure for the diffusion-controlled case ($p_g = 1$) shown by the dashed line. The dynamics of bubble pressure shown in this figure are the result of solute transport from the liquid to the gas phase occurring at a rate faster than the rate of increase of bubble volume. At early stages of the process, bubble growth is inhibited and, consequently, the

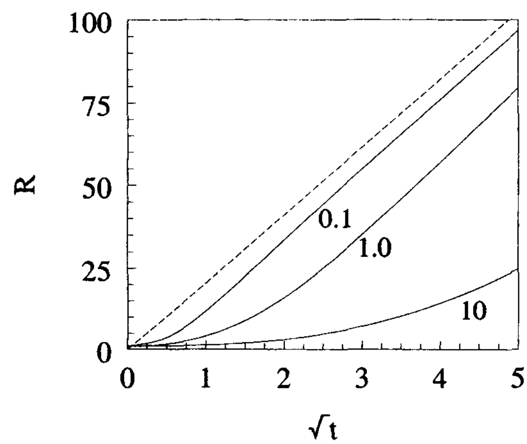

Figure 1. Bubble growth dynamics from rigorous model for $N_A = 10$ and values of N_T indicated in figure.

Values of other dimensionless groups are given in Table 1. Dashed line corresponds to diffusion-controlled case where $N_T = N_C = N_R = 0$ and $R(0) = 0$ described by Eq. 16.

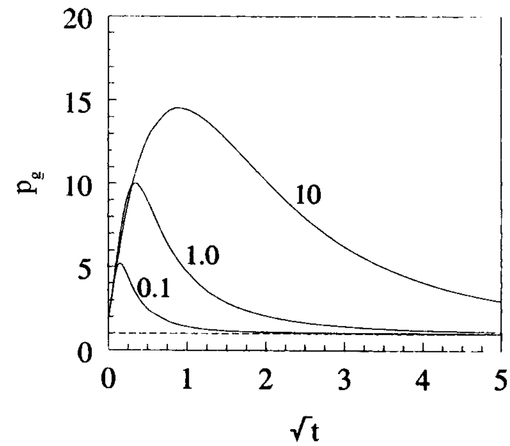

Figure 2. Bubble pressure during growth from rigorous model for $N_A = 10$ and values of N_T indicated in figure.

Values of other dimensionless groups are given in Table 1. Dashed line corresponds to diffusion-controlled case where $N_T = N_C = N_R = 0$ and $R(0) = 0$ described by Eq. 16.

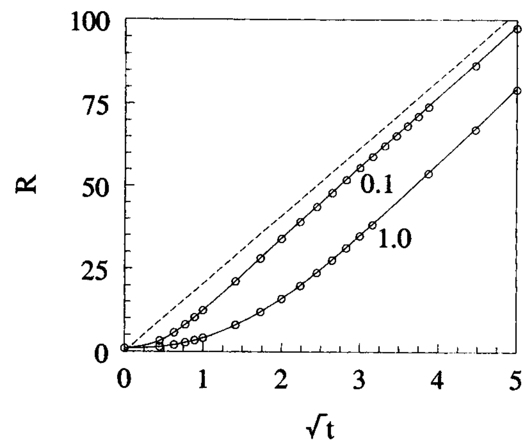

Figure 4. Comparison of bubble growth models for $N_A = 10$ and values of N_T indicated in figure.

Solid lines for rigorous model; symbols for IDS approximations model. Values of other dimensionless groups are given in Table 1. Dashed line corresponds to diffusion-controlled case where $N_T = N_C = N_R = 0$ and $R(0) = 0$ described by Eq. 16.

pressure inside the bubble must increase. As the bubble grows to a larger size, the magnitude of retarding viscous forces in the liquid surrounding the bubble diminish so that the bubble volume can increase at exactly the rate required to accommodate solute as it enters the bubble. The dynamics of p_g shown in Figure 2 and the solute boundary condition given in Eq. 5 also provide a simple explanation for the bubble growth behavior shown in Figure 1. Clearly, the driving force for mass diffusion is reduced when $p_g > 1$, further slowing the growth process.

Comparison of rigorous and approximate models

Figures 3, 4 and 5 show comparisons of bubble growth dynamics predicted by the IDS approximation model (symbols) with those from rigorous model (solid lines) for three different growth rates (N_A) with varying levels of viscous effects (N_T). For $N_A = 1.0$ shown in Figure 3 and for $N_A = 10$ shown in Figure 4, the IDS approximation is valid throughout the entire growth process for the two values of N_T shown in these figures. This is not surprising since the IDS approximation requires $N_B \ll 1$, and in Figure 3, $N_B = 0.001$, and in Figure 4, $N_B = 0.01$ (recall: N_B/N_A is fixed and equal to 0.001). For the highest growth rate, $N_A = 100$ shown in Figure 5, the IDS approximation begins to fail and results in an underprediction of the growth rate as the process approaches diffusion-controlled behavior. Hence, it appears the IDS approximation will be valid when $N_B \lesssim 0.1$.

The interaction of viscous effects and bubble growth rate can be ascertained from the rigorous model predictions in

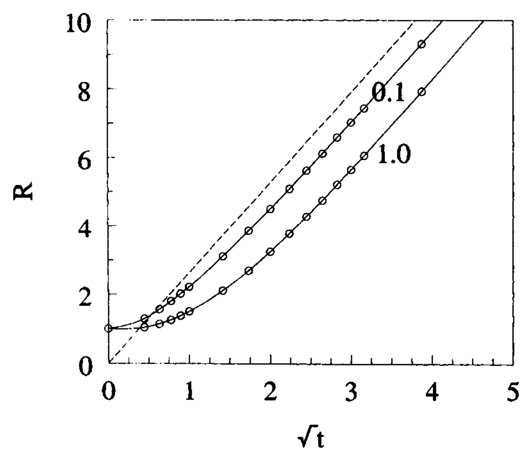

Figure 3. Comparison of bubble growth models for $N_A = 1$ and values of N_T indicated in figure.

Solid lines for rigorous model; symbols for IDS approximations model. Values of other dimensionless groups are in Table 1. Dashed line corresponds to diffusion-controlled case where $N_T = N_C = N_R = 0$ and $R(0) = 0$ described by Eq. 16.

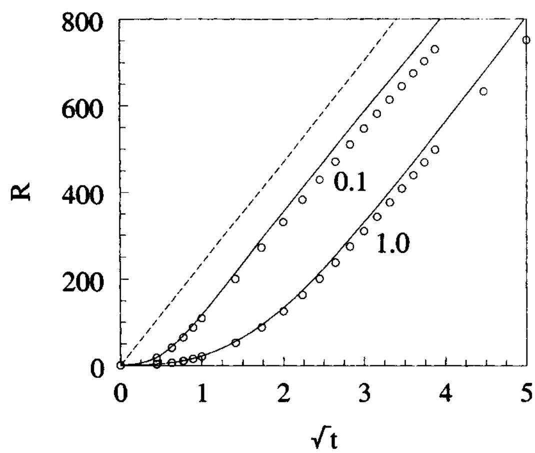

Figure 5. Comparison of bubble growth models for $N_A = 100$ and values of N_T indicated in figure.

Solid lines for rigorous model; symbols for IDS approximations model. Values of other dimensionless groups are in Table 1. Dashed line corresponds to diffusion-controlled case where $N_T = N_C = N_R = 0$ and $R(0) = 0$ described by Eq. 16.

Figures 3, 4 and 5. From these figures, it is evident that as the bubble growth rate is increased (increasing N_A) the retarding effect of viscous forces in the liquid surrounding the bubble is amplified leading to greater departures from the diffusion-controlled case shown by the dashed line. This is an important point since in practical situations where bubble growth in viscous liquids takes place, a relatively large driving force (N_A) is required in order for appreciable changes in the bubble radius to occur in reasonably short time scales.

In Figures 6, 7 and 8, predictions from the model using both the IDS and TBL approximations are compared with the predictions from the rigorous model for several different growth rates. From Figure 6 where $N_A = 1.0$, it is evident that the approximate model dramatically underpredicts the bubble growth rate. Since $N_B = 0.001$, the IDS approximation will be valid for this case (see Figure 3) so that the discrepancies between approximate (symbols) and rigorous (solid lines) models shown in Figure 6 are the result of using the TBL approximation. This is not surprising since the TBL approximation, as was mentioned in the previous section, is valid only if $N_A \gg 1$ and in this case $N_A = 1$. It is interesting to note that in two previous studies where TBL approximations have been used (Barlow and Langlois, 1962; Han and Yoo, 1981), the systems considered result in values for N_A that were on the order of one. In Figure 7 where $N_A = 10$, the agreement between the approximate and rigorous model predictions is significantly improved. However, as in Figure 8, when the growth rate is further increased, deviations between the rigorous and approximate models are observed. The discrepancies in Figure 8 can be explained by the fact that while the TBL approximation is most likely valid for this case ($N_A = 100 \gg 1$), the IDS approximation is beginning to break down since $N_B = 0.1$. Hence, as anticipated, models that use both IDS and TBL approximations are likely to have a rather limited range of applicability requiring: $0.1 \lesssim N_A N_B \lesssim 10$.

As was discussed in the previous section, diffusion-controlled bubble growth ($p_g = 1$) will be observed in viscous liquids in the limit $R \to \infty$. The results shown in Figures 3 to 8 demonstrate that during later stages of the growth process, predictions from both the rigorous model and the approximate models approach this behavior such that

$$\frac{dR}{d\sqrt{t}} = 2C \tag{42}$$

where C is a constant. It is also evident that the time or, more precisely, the bubble size required for this limiting behavior to be reached increases with increasing N_T. For all cases considered, the growth rate in the diffusion-controlled regime predicted by the rigorous model (solid lines) agrees

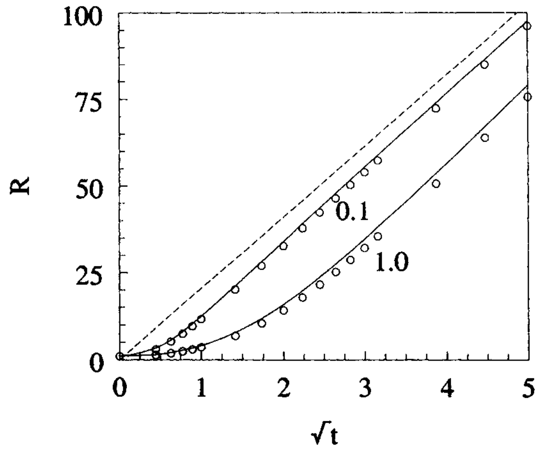

Figure 7. Comparison of bubble growth models for N_A = 10 and values of N_T indicated in figure.

Solid lines for rigorous model; symbols for IDS and TBL approximations model. Values of other dimensionless groups are given in Table 1. Dashed line corresponds to diffusion-controlled case where $N_T = N_C = N_R = 0$ and $R(0) = 0$ described by Eq. 16.

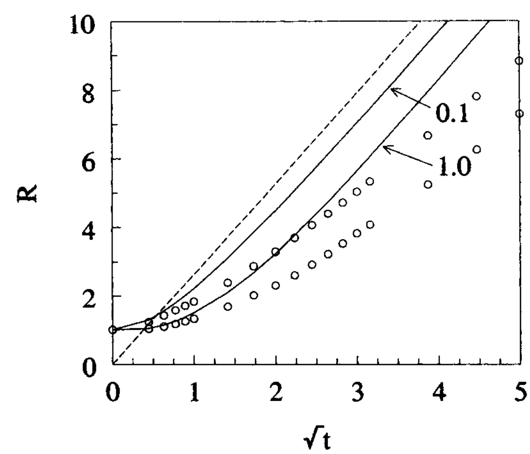

Figure 6. Comparison of bubble growth models for N_A = 1 and values of N_T indicated in figure.

Solid lines for rigorous model; symbols for IDS and TBL approximations model. Values of other dimensionless groups are given in Table 1. Dashed line corresponds to diffusion-controlled case where $N_T = N_C = N_R = 0$ and $R(0) = 0$ described by Eq. 16.

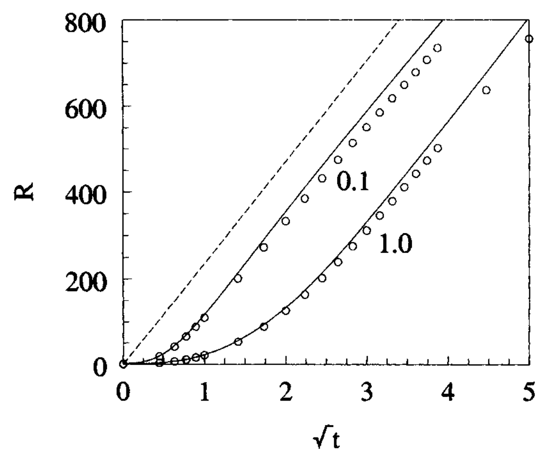

Figure 8. Comparison of bubble growth models for N_A = 100 and values of N_T indicated in figure.

Solid lines for rigorous model; symbols for IDS and TBL approximations model. Values of other dimensionless groups are given in Table 1. Dashed line corresponds to diffusion-controlled case where $N_T = N_C = N_R = 0$ and $R(0) = 0$ described by Eq. 16.

with the growth rate predicted by the exact similarity solution (dashed lines).

It appears the validity of models for bubble growth in viscous liquids using the IDS approximation, the TBL approximation, or both, can be established for later stages of the growth process by comparing predicted growth rate constants C with the exact similarity solution for diffusion-controlled bubble growth from a zero initial radius.

Comparing the exact similarity solution Eq. 16 and Eq. 42, it is evident that $C = \beta$. The TBL approximation model derived using the perturbation method, which also uses the IDS approximation, gives the following estimate for the growth rate constant

$$C = N_A \sqrt{\frac{3}{\pi}} \approx N_A \tag{43}$$

which will correspond to the diffusion-controlled behavior predicted by the models developed by Barlow and Langlois (1962) and Street et al. (1971).

The three approximate models based on the integral method considered in the previous section all approach diffusion-controlled behavior for $R \to \infty$. Equation 34 with $p_g = 1$ and $R \gg 1$ gives the following for the growth rate constant

$$C = \frac{N_A}{\sqrt{1 - N_B}} \tag{44}$$

The result in Eq. 44 was shown to be in good agreement with the exact similarity solution for $N_A \gg 1$ and $N_B/N_A \ll 1$, which ensures $\delta/R \ll 1$ in Eq. 33 for $p_g = 1$ and, hence, the validity of the TBL approximation (Rosner and Epstein, 1972). It is also evident that for $N_B \ll 1$, Eq. 44 is in approximate agreement with Eq. 43. From the improved TBL approximation, Eq. 35, with $p_g = 1$ and $R \gg 1$, we find

$$C = \sqrt{\frac{N_A}{\sqrt{1 + 2(1 - N_B)/N_A} - 1}} \tag{45}$$

At later stages of the growth process $R \to \infty$, the model of Han and Yoo (1981) will have a growth rate constant given by Eq. 45 with $N_B = 0$, since the IDS approximation was also used. From the approximate model developed by Payvar (1987), we have from Eq. 39 with $p_g = 1$ and $R \gg 1$

$$C = \sqrt{\frac{N_A}{2}\left(1 + \frac{1}{\sqrt{1 + (1 - N_B)/N_A} - 1}\right)} \tag{46}$$

The growth rate constant C for diffusion-controlled growth from the approximate models Eqs. 44–46 are compared to the exact solution $C = \beta$ in Figure 9 over a wide range of N_A with the ratio N_B/N_A fixed at 0.001. From this figure, it is evident that the TBL approximation Eq. 44 based on the integral method of Rosner and Epstein (1972) is valid only if $N_A \gtrsim 10$; that the higher-order approximation given in Eq. 45 increases the range of validity slightly to $N_A \gtrsim 3$. The approximate solution derived by Payvar (1987) given by Eq. 46 appears to be valid over the entire range of N_A shown in Figure 9. In fact, for $N_A \ll 1$; $N_B \ll N_A$, Eq. 46 reduces to

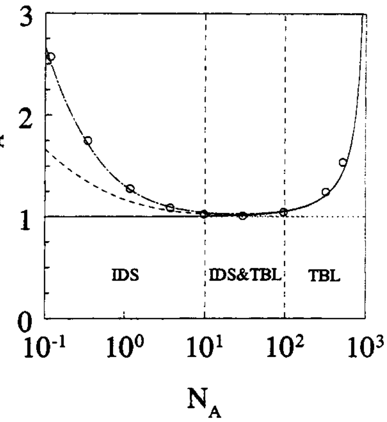

Figure 9. Comparison of growth rate constants for diffusion-controlled bubble growth from approximate models with exact solution for $N_B/N_A = 0.001$.

Symbols are for exact similarity solution; solid line for Eq. 44; dashed line for Eq. 45; dash-dot line for Eq. 46; dotted line for Eqs. 44–46 with $N_B = 0$ for $N_A > 10$. Note that solid, dashed and dash-dot lines coincide for $N_A > 100$.

$$C = \sqrt{\frac{N_A}{2}} \tag{47}$$

which is consistent with the zero-order perturbation solution for slow bubble growth (Vrentas et al., 1983). From Figure 9, it is also evident that the IDS approximation is valid for $N_A \lesssim 100$, or for $N_B \lesssim 0.1$, since N_B/N_A is fixed at 0.001. Consequently, when the IDS approximation and the TBL approximation based on the perturbation method or the integral method are both used, the range of validity of the resulting model will be rather narrow: $10 \lesssim N_A \lesssim 100$. For the improved integral method proposed by Han and Yoo (1981), the range is slightly larger: $3 \lesssim N_A \lesssim 100$. Clearly, if the ratio N_B/N_A is increased (or decreased), the upper limit on the range of applicability will decrease (or increase).

The ranges of validity for the IDS and TBL approximations established in Figure 9 are, as noted above, only applicable to later stages of bubble growth for bubbles growing in viscous liquids. One way to examine the validity of these approximations during early stages of the growth process where viscous effects are still prevalent is to make comparisons such as those shown in Figures 3 to 8. For the TBL approximation based on the integral method, the magnitude of the righthand side of Eq. 33 can be used to determine the effect momentum transport has on the validity of this approximation since it requires $\delta/R \ll 1$. As shown in Figure 2, viscous effects result in a rather dramatic increase in the bubble pressure at early stages of growth. It is evident that when $p_g > 1$, the righthand side of Eq. 33 becomes larger and, consequently, the TBL approximation ($\delta/R \ll 1$) will have a reduced range of validity as compared with the diffusion-controlled case ($p_g = 1$).

Since the approximate solution derived by Payvar (1987) given in Eqs. 37 and 38 appears to have a rather broad range of applicability, we shall use this solution to develop a model for bubble growth in viscous liquids. Recall that the model developed by Payvar (1987) used the IDS approximation ($N_B = 0$) and neglected interfacial, viscous and inertial forces in the liquid, but allowed for a time-dependent pressure in the liquid far from the bubble p_∞. This is equivalent to setting p_g equal to an arbitrary, but known function of time, and integrating Eq. 39 with $N_B = 0$.

New approximate model

The model proposed here will use the approximate solution of Payvar (1987), but will allow for interfacial, viscous and inertial forces in the liquid to surround the bubble. It also uses the IDS approximation so we can expect the model to be valid for all N_A and $N_B \lesssim 0.1$, which will include most situations of interest. Equations 21 and 39 (with $N_B = 0$) must be integrated with initial conditions in Eqs. 9, 10 and 22. To handle the singularity in Eq. 39 at $t = 0$, we integrate this equation over a small time step from $t = 0$ to $t = \Delta t$, where it is assumed that bubble radius remains fixed, which results in a small jump in the bubble pressure from $p_g(0)$ to $p_g(\Delta t)$. This mathematical approximation can be justified from physical arguments since inertial effects in the liquid, however small, will prevent the liquid surrounding the bubble from accelerating instantaneously. Hence, a small amount of solute will diffuse into the bubble, whose radius is momentarily fixed, causing a jump in the bubble pressure. The proposed model is given by the following set of ordinary differential equations, derived from Eqs. 21 and 39 with $N_B = 0$, along with initial conditions modified to resolve the singularity

$$\frac{dR}{dt} = \dot{R} \qquad R(\Delta t) = 1 \tag{48}$$

$$\frac{d\dot{R}}{dt} = \frac{1}{N_R}\left[p_g - \left(1 + 2\frac{N_C}{R}\right) - 4N_T\frac{\dot{R}}{R}\right]\frac{1}{R} - \frac{3}{2}\frac{\dot{R}^2}{R} \qquad \dot{R}(\Delta t) = 0 \tag{49}$$

$$\frac{dp_g}{dt} = -3p_g\frac{\dot{R}}{R} + 3\frac{N_A}{R^2}\left(\frac{1 - N_K p_g}{1 - N_K}\right) \times \left[1 + \left(\sqrt{1 + \frac{1}{N_A}\frac{1 - N_K}{1 - N_K p_g}\frac{p_g R^3 - (1 + 2N_C)}{R^3}} - 1\right)^{-1}\right] \tag{50}$$

$$p_g(\Delta t) = 1 + 2N_C + 2N_A\sqrt{3\Delta t}$$

Note that the time step Δt appearing in Eqs. 48–50 can be made arbitrarily small so that the initial conditions given in Eqs. 9, 10 and 22 are recovered.

Figure 10 shows a comparison of bubble growth behavior from the proposed model (filled symbols) and the rigorous model (solid line) for $N_A = 1$ and $N_T = 1$. This figure shows that the proposed approximate model given by Eqs. 48–50 is in fairly good agreement with the rigorous model given by Eqs. 1–11. Comparisons of the proposed approximate model and the rigorous models for other growth rates showed similar results. Thus, it appears that reasonably accurate predictions can be achieved while significantly reducing computational effort—solving three ordinary differential equations rather than solving a system of ordinary and partial differential equations. Also shown in Figure 10 are predictions from the model using the TBL approximation derived by Rosner and Epstein (1972) (Eq. 41). Based on the results shown in Figure 9, it can be expected that the improved TBL approximation model suggested by Han and Yoo (1981), Eq. 34 with $N_B = 0$, will give predictions somewhere between the filled and open symbols shown in Figure 10. To make these comparisons somewhat more quantitative, let t_{10} be the time required for a bubble to grow to ten times its initial size: $R(t_{10}) = 10$. For the case shown in Figure 10, the prediction from the TBL approximation model predicts a value of t_{10} that is off by a factor of about three, while the approximate model given by Eqs. 48–50 is off by about 6.5%. From Figure 9, it appears that at higher growth rates (larger N_A), discrepancies between the two approximate models and between the approximate models and the rigorous model will diminish until $N_B \gtrsim 0.1$. At lower growth rates (smaller N_A), we can expect the approximate model given by Eqs. 48–50 to be superior to previously-proposed models that use a TBL approximation.

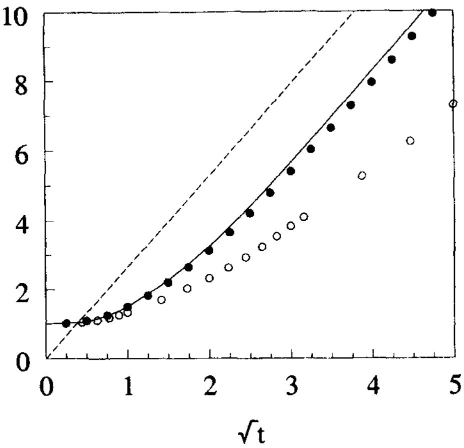

Figure 10. Comparison of bubble growth models for $N_A = 1$ and $N_T = 1$.

Solid line for rigorous model; open symbols for IDS and TBL approximations model; filled symbols for model given in Eqs. 48–50. Values of other dimensionless groups are given in Table 1. Dashed line corresponds to diffusion-controlled case where $N_T = N_C = N_R = 0$ and $R(0) = 0$ described by Eq. 16.

Summary

A rigorous transport model for bubble growth and dissolution in viscous liquids has been formulated. We have shown how previously proposed, approximate models of these phenomena can be derived from the rigorous model using various mathematical methods. Two simplifying approximations have been used extensively in previous modeling work without validation—the infinitely dilute solute (IDS) and the thin boundary-layer (TBL) approximations. Using dimensional analysis, we have shown that the IDS approximation corresponds to $N_B \ll 1$ and the TBL approximation corresponds to $N_A \gg 1$, where N_B is a dimensionless group related to the driving force for mass diffusion and N_A is a dimensionless group related to the rate of bubble growth.

The retarding effect of viscous forces on bubble growth rate has been examined and is explained by a rather dramatic increase in the bubble pressure at early stages of the growth process, which also reduces the effective concentration difference that drives mass diffusion. This retarding effect was shown to be more pronounced at higher growth rates.

Comparison of bubble growth behavior predicted by the rigorous model with predictions from approximate models using the IDS approximation and using both the IDS and TBL approximations have been carried out over a wide range of conditions. Good agreement between the rigorous model and the IDS approximation model was found when $N_B \lesssim 0.1$. For the model using both the IDS and TBL approximations, good agreement was found over a relatively limited range: $0.1 \lesssim N_A N_B \lesssim 10$.

Although predictions for bubble collapse were not presented, it is expected that the IDS approximation will be valid when $|N_B| \lesssim 0.1$. Based on results for diffusion-controlled bubble collapse where the TBL approximation is limited to $|N_A| \geq 100$ (Vrentas et al., 1983), we can expect similar restrictions on models for diffusion-induced bubble collapse in viscous liquids.

A new approximate model for bubble growth in viscous liquids has been formulated based on a previously-published, approximate solution of the species continuity equation that does not require a TBL approximation. Predictions from this approximate model, which requires integration of three ordinary differential equations, were found to be in reasonably good agreement with predictions from the rigorous model, which requires considerably more computational effort.

The results of this study should provide a firmer foundation for the development of more realistic (complex) models for diffusion-induced bubble growth and collapse in viscous liquids. For example, non-Newtonian fluids can be handled by appropriate modification of the integrated momentum balance on the liquid. Elasticity and other non-Newtonian effects will be the subject of a forthcoming article.

Acknowledgment

The financial support provided by the Amoco Foundation to the Center of Excellence in Polymer Science and Engineering for this study is gratefully acknowledged.

Notation

$A = M_1/RT$ = solute gas density factor where: M_1 is solute molecular weight, R is the ideal gas law constant, and T is the absolute temperature

$p_g = p_g^*/p_\infty$ = dimensionless bubble pressure

$r = r^*/R_0$ = dimensionless radial coordinate

$R = R^*/R_0$ = dimensionless bubble radius

$t = t^* D/R_0^2$ = dimensionless time

$v_r = v_r^* R_0/D$ = dimensionless radial velocity

$\rho_1 = \dfrac{\rho_1^* - \rho_{10}}{\rho - kp_\infty}$ = dimensionless solute mass density

Literature Cited

Amon, M., and C. D. Denson, "A Study of the Dynamics of Foam Growth: Analysis of the Growth of Closely Spaced Spherical Bubbles," *Poly. Eng. Sci.*, **24**(13), 1026 (1984).

Arefmanesh, A., and S. G. Advani, "Diffusion-Induced Growth of a Gas Bubble in a Viscoelastic Liquid," *Rheol. Acta*, **30**, 274 (1991).

Arefmanesh, A., S. G. Advani, and E. E. Michaelides, "A Numerical Study of Bubble Growth During Low Pressure Structural Foam Molding Process," *Poly. Eng. Sci.*, **30**(20), 1330 (1990).

Arefmanesh, A., S. G. Advani, and E. E. Michaelides, "An Accurate Numerical Solution for Mass Diffusion-Induced Growth in Viscous Liquids Containing Limited Dissolved Gas," *Int. J. Heat Mass Transfer*, **35**, 1711 (1992).

Barlow, E. J., and W. E. Langlois, "Diffusion of Gas from a Liquid into an Expanding Bubble," *IBM J.*, 329 (July 1962).

Duda, J. L., and J. S. Vrentas, "Mathematical Analysis of Bubble Dissolution," *AIChE J.*, **15**(3), 351 (1969).

Epstein, P. S., and M. S. Plesset, "On the Stability of Gas Bubbles in Liquid-Gas Solutions," *J. Appl. Phys.*, **18**(11), 1505 (1950).

Han, C. D., and H. J. Yoo, "Studies on Structural Foam Processing: IV. Bubble Growth During Mold Filling," *Poly. Eng. Sci.*, **21**(9), 518 (1981).

Patel, R. D., "Bubble Growth in a Viscous Newtonian Liquid," *Chem. Eng. Sci.*, **35**, 2352 (1980).

Payvar, P., "Mass Transfer-Controlled Bubble Growth During Rapid Decompression of a Liquid," *Int. J. Heat Mass Transfer*, **30**(4), 699 (1987).

Plesset, M. S., and S. A. Zwick, "A Nonsteady Heat Diffusion Problem with Spherical Symmetry," *J. Appl. Phys.*, **23**(1), 95 (1952).

Ramesh, N. S., D. H. Rasmussen, and G. A. Campbell, "Numerical and Experimental Studies of Bubble Growth During the Microcellular Foaming Process," *Poly. Eng. Sci.*, **31**, 1657 (1991).

Rosner, D. E., and M. Epstein, "Effects of Interface Kinetics, Capillarity and Solute Diffusion on Bubble Growth Rates in Highly Supersaturated Liquids," *Chem. Eng. Sci.*, **27**, 69 (1972).

Scriven, L. E., "On the Dynamics of Phase Growth," *Chem. Eng. Sci.*, **10**, 1 (1959).

Street, J. R., A. L. Fricke, and L. P. Reiss, "Dynamics of Phase Growth in Viscous, Non-Newtonian Liquids," *Ind. Eng. Chem. Fundam.*, **10**(1), 54 (1971).

Szekely, J., and G. P. Martins, "Non-Equilibrium Effects in the Growth of Spherical Gas Bubbles Due to Solute Diffusion," *Chem. Eng. Sci.*, **26**, 147 (1971).

Villamizar, C. A., and C. D. Han, "Studies on Structural Foam Processing II. Bubble Dynamics in Foam Injection Molding," *Poly. Eng. Sci.*, **18**(9), 699 (1978).

Vrentas, J. S., C. M. Vrentas, and H.-C. Ling, "Equations for Predicting Growth and Dissolution Rates of Spherical Particles," *Chem. Eng. Sci.*, **38**(11), 1927 (1983).

Yoo, H. J., and C. D. Han, "Oscillatory Behavior of a Gas Bubble Growing (or Collapsing) in Viscoelastic Liquids," *AIChE J.*, **28**(6), 1002 (1982).

Zana, E., and L. G. Leal, "Dissolution of a Stationary Gas Bubble in a Quiescent, Viscoelastic Liquid," *Ind. Eng. Chem. Fundam.*, **14**(3), 175 (1975).

Manuscript received Mar. 7, 1997, and revision received July 3, 1997.